Journal of Catalysis **184,** 236–246 (1999)
Article ID jcat.1999.2450, available online at http://www.idealibrary.com on

Vanadium Nitride Catalysts: Synthesis and Evaluation for *n*-Butane Dehydrogenation

H. Kwon, S. Choi, and L. T. Thompson[1]

Department of Chemical Engineering, University of Michigan, Ann Arbor, Michigan 48109-2136

Received October 30, 1998; revised December 30, 1998; accepted January 30, 1999

A series of mesoporous vanadium nitrides with surface areas up to 60 m^2/g was prepared via the temperature-programmed reaction of V_2O_5 with NH_3, and evaluated for the dehydrogenation of *n*-butane. Thermogravimetric analysis coupled with X-ray diffraction and scanning electron microscopy indicated that the solid-state reaction proceeded by the sequential reduction of V_2O_5 ($V_2O_5 \rightarrow V_4O_9 \rightarrow VO_2 \rightarrow V_2O_3 \rightarrow VO_{0.9}$) and concluded with the topotactic substitution of nitrogen for oxygen in $VO_{0.9}$. An experimental design was performed to determine effects of the heating rates and space velocities on the VN microstructures. The heating rates had minor effects on the surface areas and pore size distributions; however, increasing the space velocity significantly increased the surface area and decreased the average pore size. We believe the effect of the space velocity was due to inhibition of the gas–solid reactions by H_2O and/or N_2. Temperature-programmed reduction and pretreatment studies indicated that the passivated VN could be activated by reduction in H_2 at 500°C for 3 h. Lower reduction temperatures or times resulted in suppressed surface areas and O_2 chemisorptive uptakes. Oxygen chemisorption on the fully reduced vanadium nitrides scaled linearly with the surface area. The corresponding $O/V_{surface}$ ratio was 0.56 suggesting that each oxygen atom chemisorbed to approximately two surface vanadium atoms. The vanadium nitrides were highly active butane dehydrogenation catalysts with selectivities in excess of 98%. Volumetric reaction rates for the highest surface area VN were superior to those for a Pt–Sn/Al_2O_3 catalyst. The average turnover frequency for the VN catalysts was $4.3 \times 10^{-4}\ s^{-1}$ at 450°C assuming that oxygen chemisorbed atomically onto the active sites. The corresponding turnover frequency for the Pt–Sn/Al_2O_3 catalyst was $6.3 \times 10^{-2}\ s^{-1}$ suggesting that while selectivities for the VN and Pt–based catalysts were similar, VN had a lower intrinsic activity. © 1999 Academic Press

INTRODUCTION

Early transition metal nitrides and carbides have been demonstrated to be active and selective for reactions including hydrodenitrogenation (1–3), CO oxidation (4), NH_3 synthesis (5), and butane hydrogenolysis and isomerization (6, 7). Of particular interest here are reports that the catalytic properties of some early transition metal nitrides and carbides are similar to those of noble metals. For example, Mo_2C catalyzes CO hydrogenation with activities approaching that of Ru (4) and W_2C exhibits Pt-like behavior for the isomerization of 2,2-dimethylpropane (8). Recently we examined the activity and selectivity patterns of Group V and VI metal nitrides and carbides for several hydrocarbon activation reactions. Results for the activation of butane are summarized in Table 1 (7). Surface areas for these materials were relatively low and no attempt was made to optimize their performance. Except for NbN and NbC, all of the materials were active with reaction rates that were comparable to or greater than that for a Pt–Sn/Al_2O_3 catalyst. The surface area normalized reaction rates ranged up to 171 nmol/m^2 s at 450°C and decreased in the following order: $Mo_2N > W_2C \approx WC > W_2N \approx WC_{1-x} > Mo_2C > VN \approx VC > NbN \approx NbC$. The metal atom type had the most significant effect while effects of the nonmetal atom type were relatively small. The Group VI compounds were much more active than the Group V metal nitrides and carbides; however, selectivities for the Group VI materials were poor. At similar conversions, the Group VI transition metal nitrides and carbides catalyzed alkane hydrogenolysis, dehydrogenation, and isomerization while the Group V compounds selectively catalyzed the dehydrogenation reactions. Results for the vanadium compounds were qualitatively consistent with reports by Chen *et al.* (9) that VC was active for the dehydrogenation of isobutane. With sufficient increases in their surface areas, vanadium nitrides and carbides could be competitive catalysts for the selective dehydrogenation of alkanes.

The goal of research described in this paper was to prepare high surface area vanadium nitrides and assess their ability to catalyze *n*-butane dehydrogenation. Temperature-programmed reaction (TPR) methods similar to those developed by Boudart and co-workers to prepare other high surface area early transition metal nitrides and carbides were used (10–12). We investigated solid-state reactions that occurred during the TPR of V_2O_5 with NH_3 using thermogravimetric analysis (TGA), X-ray diffraction

---

[1] To whom correspondence should be addressed: Department of Chemical Engineering, University of Michigan, 3026 H. H. Dow Building, Ann Arbor, MI 48109-2136. E-mail: ltt@umich.edu.

0021-9517/99 $30.00

TABLE 1

Catalytic Properties of the Group V and VI Transition Metal Nitrides and Carbides[a] (7)

Catalyst	Surface area (m^2/g)	Gravimetric reaction rates (nmol/g s)				Activity ($nmol/m^2$ s)
		Dehydrogenation	Isomerization	Hydrogenolysis	Total	
VN	14	89	<0.1	<0.1	89	6.4
VC	11	64	<0.1	<0.1	64	5.8
NbN	33	<0.1	<0.1	<0.1	<0.1	<0.01
NbC	30	<0.1	<0.1	<0.1	<0.1	<0.01
Mo_2N	21	2021	91	1644	3760	171
Mo_2C	63	1300	9.0	703	2013	32
W_2N	81	2348	2389	1122	5855	72
WC	12	365	25	750	1141	95
W_2C	18	506	42	1470	2021	112
WC_{1-x}	48	1060	108	1539	2713	57
Pt-Sn/Al_2O_3	228	350	1.1	2.9	354	—

[a] Reaction rates measured at 450°C and 101 kPa for a reactant mixture containing 4% n-C_4H_{10}, 60% H_2, and 36% He.

(XRD), and scanning electron microscopy (SEM). Our results concerning the solid-state reaction pathways are different from those reported by Oyama and co-workers (13) who used product gas analysis and XRD to track development of the nitride. These differences will be discussed. We also executed experimental designs to systematically determine effects of the heating rates and space velocities on the vanadium nitride surface areas, crystallite sizes, and pore size distributions. The surface areas and chemisorptive uptakes were significantly influenced by the conditions used to activate the passivated vanadium nitrides. Temperature programmed reduction studies were instrumental in determining conditions for removing the passivation layer. Finally, the *n*-butane dehydrogenation rates and selectivities of vanadium nitrides with varying surface areas were evaluated. To the best of our knowledge this is the first report of its kind. The results allow us to provide tentative correlations between the catalytic and microstructural properties of high surface area vanadium nitrides.

EXPERIMENTAL

Synthesis

The vanadium nitrides were synthesized by reacting V_2O_5 (99.95%, Alfa) with NH_3 (99.998%, Scott) in a temperature programmed manner. The oxide had a BET surface area of 7 m^2/g. Approximately 3 g of the oxide were used for each run. The reaction temperatures were selected based on results from thermogravimetric analysis of the reaction of V_2O_5 and NH_3. Details concerning the synthesis reactor system are given elsewhere (14). The molar hourly space velocity, defined as the ratio of the molar flow rate of NH_3 to the moles of V_2O_5, was varied in an attempt to vary the nitride microstructure. After synthesis, the furnace was opened and the product was rapidly cooled in flowing NH_3, purged with He for 10 min, and then passivated using a mixture of 1% O_2 in He (Scott) flowing at 20 ml/min for 2 h. After passivation, the product was taken out of the reactor and stored in an evacuated desiccator for subsequent characterization and evaluation.

A Cahn Model TG-171 thermogravimetric analyzer was used to acquire the TGA patterns. Approximately 100–400 mg of V_2O_5 powder was placed in a quartz sample holder. The sample holder was suspended from the end of a ceramic rod connected to the microbalance. A K-type thermocouple (Chromel-Alumel, Omega) was placed beneath the sample holder. The NH_3 flow rate was set at 40 ml/min. Since the NH_3 did not flow through the powder, the space velocity is not that meaningful; nevertheless, the NH_3 flow rate would correspond to space velocities of 50–200 h^{-1} depending on the sample weights. Solid intermediates produced as V_2O_5 reacted with NH_3 were collected by stopping the TGA run, recovering the product, and characterizing this material using XRD and SEM. All of the intermediates were passivated by slowly leaking air into the TGA reactor prior to removal from the system.

Characterization

The surface areas were measured by the single point BET method using a Quantasorb Model QS-17 sorption analyzer. Prior to measuring the surface areas via N_2 adsorption at −196°C, the materials were pretreated in H_2 (99.99%, Air Products) in order to remove the passivation layer and other impurities then purged with He. Reduction of the passivation layer was investigated via the temperature-programmed reduction of selected materials. An Altamira AMI-M catalyst characterization system equipped with thermal conductivity and mass spectrometer detectors was used to perform the temperature-programmed reduction experiments. Approximately 50 mg of the catalyst was placed in a quartz U-tube over a quartz wool plug. A thermocouple was placed in the bed to ensure good thermal contact with the catalyst. The nitride bed was purged with Ar (99.998%, Cryogenic) for 10 min at room temperature then heated at 5°C/min in flowing 5.2% H_2 in Ar (Cryogenic) from room temperature to 600°C, the maximum temperature for the instrument. The material was held at 600°C for several hours and then cooled to room temperature. Gas flow rates during the purge, heating, and cooling segments were $\approx$40 ml/min.

The average size of particles at the surface, d_p, was estimated from the surface area using the equation

$$d_p = \frac{6}{S_g \rho},$$

where S_g is the BET surface area, and ρ is the density of the material (here taken to be 6.08 g/cm^3 for VN). This equation assumes spherical and/or cubic particles. Pore size distributions were determined from N_2 adsorption/desorption isotherms measured using a Micromeritics ASAP 2010 analyzer. The samples were degassed *in vacuo* at 400°C for at least 5 h prior to measuring the isotherms at −196°C. Pore size distributions were determined using a Density Functional Theory (DFT) fitting program. Methods based on the DFT are typically adequate for determining the distribution of pores with sizes up to $\approx$400 nm (15–17).

Pulsed oxygen chemisorption was used to normalize the reaction rates. We prefer oxygen chemisorption over hydrogen chemisorption because hydrogen is much more prone to populate subsurface sites in nitrides and carbides (1, 18). Prior to the chemisorption measurements, the materials were pretreated using the same procedure that we used prior to the BET surface area measurements. Calibrated volumes of 9.98% O_2 in He (Scott) were injected into the He carrier gas entering the pretreated catalyst bed −978°C. Oxygen that was not adsorbed was detected and recorded. When the O_2 pulses reached a constant area, the surface was considered to be saturated. The amount of O_2 adsorbed was calculated from the number of pulses and the peak areas. The BET surface area and O_2 uptake measurements were replicated, and the reported values are averages.

Phase identification and crystallite size analysis were accomplished using a Rigaku DMAX-B X-ray diffractometer. The crystalline phases were identified by comparing the lattice parameters to those of standard compounds. The average crystallite size, d_c, was calculated using the Scherrer equation (19)

$$d_c = \frac{K\lambda}{B\cos\theta},$$

where K is a constant (here taken to be 0.9), λ is the wavelength of the X-radiation (1.5405 Å), B is the corrected peak width at half maximum intensity, and θ is the Bragg angle of the diffraction peak.

An S-800 Field Emission SEM (Hitachi) was employed to characterize the surface microstructures. No metal or carbon coating was required because the materials were electronically conductive. The microscope was operated at 5 kV with the chamber pressure at ca. 8×10^{-9} Torr.

Determination of Catalytic Properties

The catalytic properties were measured using a 6 mm o.d. quartz U-tube flow reactor. Between 40 and 100 mg of catalyst was loaded into the reactor on top of a plug of quartz wool and reduced in H_2. A K-type thermocouple was inserted directly into the catalyst bed. After reduction in H_2 at 500°C for 3 h, the bed was cooled to 450°C and the reactant mixture flow was initiated. The reaction rates were measured at temperatures between 375 and 475°C, and atmospheric pressure. Unless otherwise stated the reactant mixture consisted of 4% C_4H_{10}, 60% H_2, and 36% He (Scott) and the flow rate was held constant at 50 ml/min. The butane conversion did not exceed 2% so the system was treated as a differential reactor. The reaction products were separated using a 3.05 m *n*-Octane/Porasil C packed column (Alltech Associates) and analyzed using a HP 5890 Series II gas chromatograph with a flame ionization detector.

RESULTS AND DISCUSSION

Solid-State Reaction Pathway

Thermogravimetric analysis and XRD were used to isolate intermediates during the reaction of V_2O_5 with NH_3. Changes in the sample weight are indicators of solid-state transformations and/or adsorption/desorption events. Peaks in the derivative plot were used to more clearly identify these transformation temperatures. Typical TGA patterns are illustrated in Fig. 1. The small peak at $\approx$200°C is believed to be due to the desorption of H_2O and/or other adsorbates. The other transformation temperatures were functions of the heating rate employed. As the heating rate was increased from 60 to 180°C/h, the peaks shifted to higher temperatures. This type of behavior is typically a consequence of the rate-limiting process being diffusion of species into and/or out of the solid although surface reaction or desorption processes cannot be ruled out. The reaction of V_2O_5 with NH_3 commenced at $\approx$250°C and continued through four intermediates which produced peaks in the derivative plot at approximately 320, 350, 440, and 620°C when a heating rate of 60°C/h was employed.

Diffraction patterns for solid intermediates isolated by quenching the reaction at various temperatures are shown in Fig. 2. The intermediates were single phase and matched patterns found in the Powder Diffraction File (20). The structures of $VO_{0.9}$ and VN are similar; nevertheless they can be distinguished from each other using XRD because

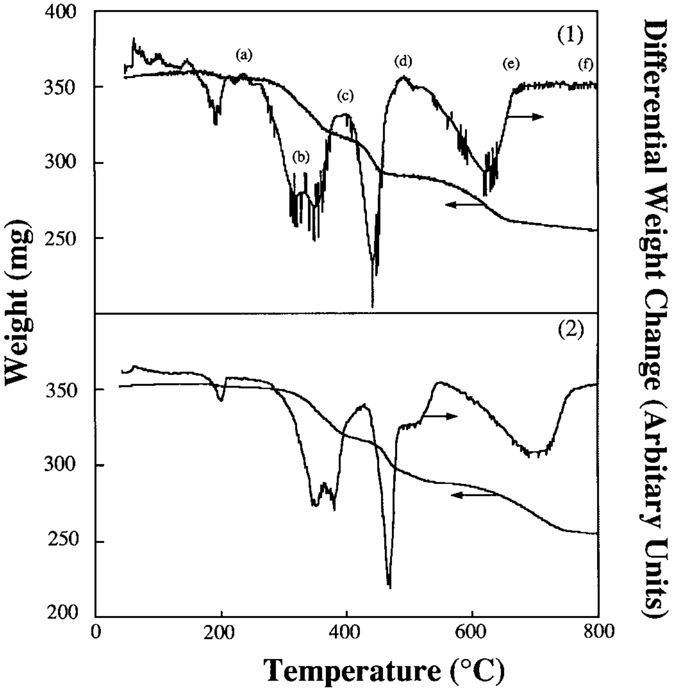

FIG. 1. Thermal gravimetric analysis of the reaction of V_2O_5 and NH_3 using heating rates of (1) 60°C/h and (2) 180°C/h.

their lattice constants are 0.406 and 0.414 nm, respectively (20). The weight changes obtained from the TGA at 60°C/h are compared to the theoretical values determined from the crystalline phases in Table 2. The reference weight was taken at point (a) where contributions from the adsorption of water and/or other species were insignificant. Weight changes during the conversion of V_2O_5 to V_2O_3, $VO_{0.9}$, and VN were within experimental error (±2%) of the respective theoretical values.

Based on the TGA and XRD results, we concluded that the TPR of V_2O_5 with NH_3 progressed sequentially to VN via V_4O_9, VO_2, and V_2O_3 and $VO_{0.9}$ intermediates. During the final stages of nitridation oxygen atoms in $VO_{0.9}$ were replaced with nitrogen. This reaction can be considered topotactic given similarities between the lattice structures of $VO_{0.9}$ and VN. In a strict sense the complete nitridation of V_2O_5 was not topotactic as it has been previously suggested (22) because lattice structures of the intermediates were significantly different. Intermediates observed in our experiments were different from those reported by Kapoor and Oyama (13). They reported the formation of V_6O_{13} and V_2O_4 prior to the production of VO_2. We did not observe V_6O_{13} or V_2O_4 in any of our experiments. Discrepancies between the results may be linked to differences between the TPR conditions and/or differences between morphologies of the oxides. Kapoor and Oyama (13) used a space velocity of 1300 h^{-1}; our nitrides were prepared using space velocities ≤ 400 h^{-1}. Previous studies of the TPR of MoO_3 with NH_3 demonstrated the strong influence of space velocity on the solid-state reaction pathway (1, 23, 24). Surface areas for the V_2O_5 powders used in our work were 7 m^2/g while Kapoor and Oyama (13) used V_2O_5 powders with 19 m^2/g to prepare their VN. One would expect the nitride surface area

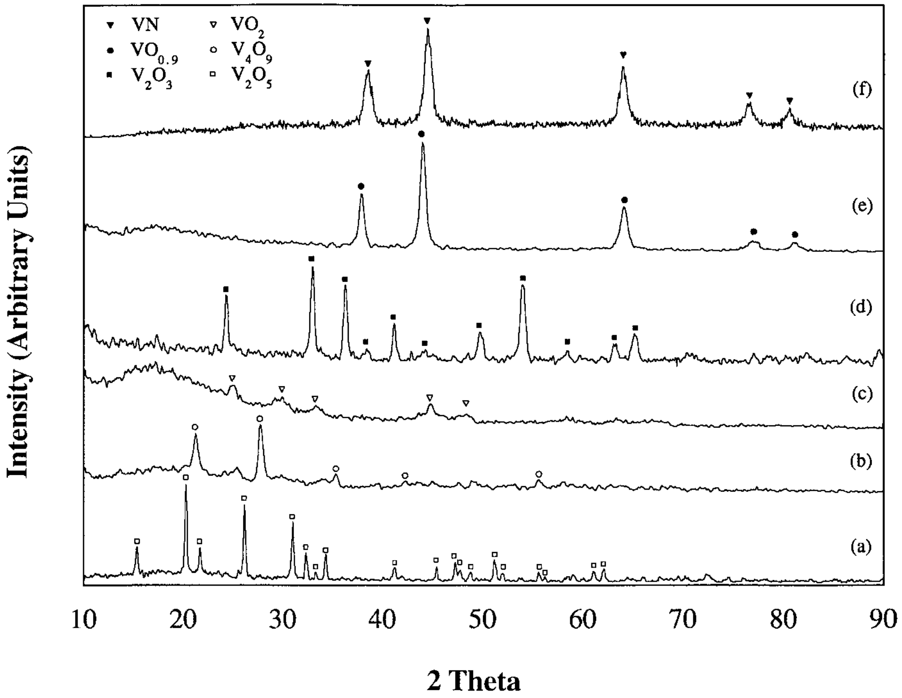

FIG. 2. X-ray diffraction patterns of products from the reaction of V_2O_5 and NH_3. These materials were collected after quenching the reaction at (a) 230, (b) 320, (c) 390, (d) 490, (e) 650, and (f) 800°C. The heating rate was 60°C/h.

TABLE 2

Weight Losses and Crystalline Phases Produced during Thermal Gravimetric Analysis[a]

Sampling point	(a)	(b)	(c)	(d)	(e)	(f)
Temperature (°C)	230	320	390	490	650	800
Actual weight loss (%)	0	5.6	11	18.1	27.2	28.1
Crystalline phase by XRD	V_2O_5	V_4O_9	VO_2	V_2O_3	$VO_{0.9}$	VN
Theoretical density[b] (g/cm^3)	3.36	3.30	4.34[c]	5.02	5.76[c]	6.08
Theoretical weight loss (%)	0	4.4	8.8	17.6	28.2	28.6

[a] The heating rate for the corresponding TGA experiments was 60°C/h.

[b] From Powder Diffraction Files (20) unless otherwise specified.

[c] From CRC Handbook (21).

and perhaps the reaction pathway to be a function of the oxide morphology. Despite the differing synthesis conditions, oxide morphologies, and reaction pathways, surface areas for nitrides produced in our work (up to 60 m^2/g) were similar to those reported by Kapoor and Oyama (up to 90 m^2/g) (13).

There were significant microstructural changes associated with the TPR of V_2O_5 and NH_3 (Fig. 3). The degree of surface roughness increased as the reduction progressed. The microstructural changes were greatest when VO_2 converted to V_2O_3. The microstructural changes continued until $VO_{0.9}$ was formed; no significant differences were observed between the microstructures of $VO_{0.9}$ and VN. We believe this latter observation was a consequence of the reaction being topotactic. Similarities between the microstructures of $VO_{0.9}$ and VN are consistent with previous reports that the surface area did not change significantly when VO transformed to VN (13). We also observed that gross morphologies of the precursor, intermediates, and product nitride were similar which implied that the overall reaction was pseudomorphic. The pseudomorphic conversion of V_2O_5 to VN would result in a substantial increase in the internal surface area due to the dramatic increase in density (see Table 2).

Effect of Synthesis Parameters on the Microstructural Properties

To evaluate effects of the space velocity, we varied the NH_3 flow rate while holding the oxide weight and temperature program constant. The oxides were heated in flowing NH_3 from room temperature to 660°C at 60°C/h. Surface areas for the materials were measured after reduction in H_2 at 500°C for 3 h. The selection of these reduction conditions will be justified in the next section. The effect of the space velocity on the surface area was significant. As the space velocity was increased, the surface areas increased to an asymptotic value (Fig. 4). For space velocities lower than 15 h^{-1}, phase-pure VN could not be produced; instead, mixtures of V_2O_3, $VO_{0.9}$, and VN were obtained. Beyond 300 h^{-1}, the surface area did not increase and therefore there was no apparent advantage to further increases in the space velocity. The nitride produced using the highest space velocity (370 h^{-1}) had a surface area almost 3 times that of the nitride produced using the lowest space velocity (20 h^{-1}). We believe this increase was due to the effect of reaction products on the surface areas. Water, nitrogen, and other reaction products could affect the surface area by inhibiting critical surface and solid-state reactions (13, 25, 26). Consider the overall reaction producing VN from V_2O_5 and NH_3.

$$V_2O_5 + 10/3NH_3 \leftrightarrow 2VN + 5H_2O + 2/3N_2$$

According to the law of mass action, H_2O and N_2 would slow the oxide reduction and/or nitridation reactions by enhancing rates for the reoxidation reactions. The net result would be higher reduction and nitridation temperatures to complete the conversion when H_2O and/or N_2 are present. Indeed it has been observed that the presence of H_2O caused the transformation of V_2O_5 to VN to shift to higher temperatures (13). The higher temperatures would enhance sintering and the loss of surface area. High space velocities would increase the mass transfer rates and facilitate the removal of H_2O, N_2, and other products from the solid surface. Consequently their partial pressures would decrease favoring the forward reactions. By reducing the H_2O vapor partial pressure, the potential for hydrothermal sintering would also be reduced (27).

The crystallite and particle sizes were similar for the high surface area nitrides; however, the crystallites were smaller than the particles for the low surface area nitrides. Deviations between the crystallite and particle sizes for these materials suggested the presence of polycrystalline particles. The vanadium nitrides yielded Type IV isotherms indicating that the materials were mesoporous. The mean pore sizes decreased from 42 to 12 nm as the space velocity was increased (Fig. 5). Furthermore, the pore size distributions were narrower for the higher surface area materials.

To study effects of the heating rates, a 2^k factorial experimental design was executed. Heating rates of 60 and/or 180°C/h were employed. The temperature profile

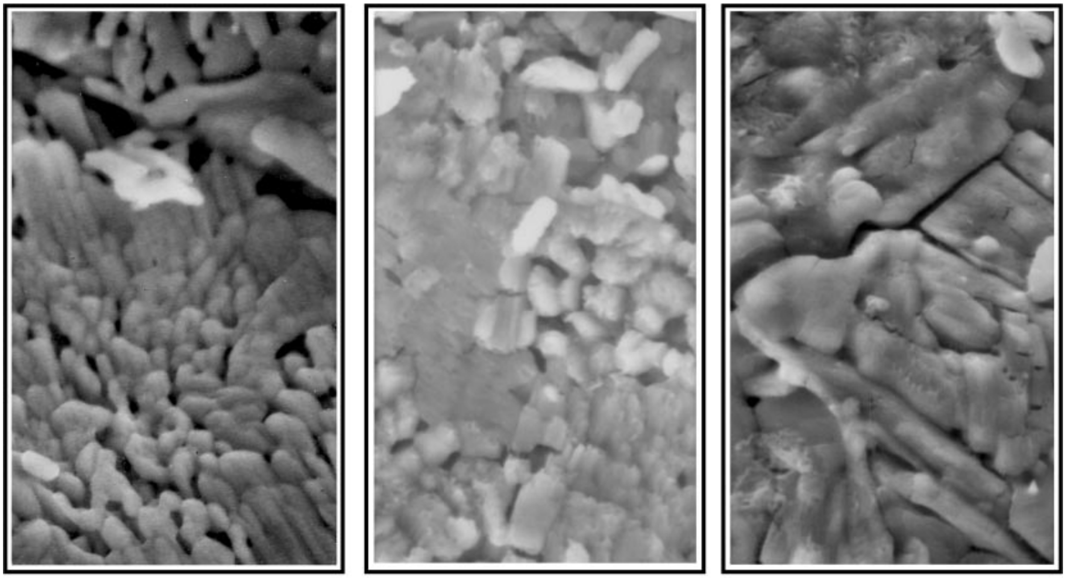

(a) V_2O_5--orthorhombic (b) V_4O_9--tetragonal (c) VO_2--tetragonal

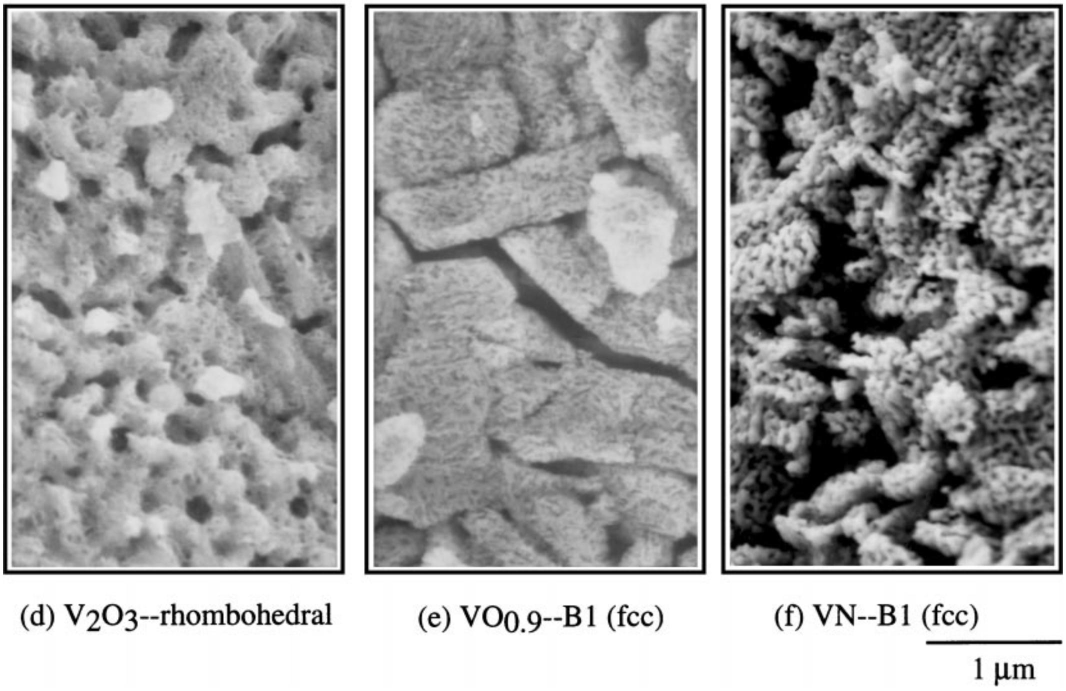

(d) V_2O_3--rhombohedral (e) $VO_{0.9}$--B1 (fcc) (f) VN--B1 (fcc)

FIG. 3. Scanning electron micrographs of products from the reaction of V_2O_5 and NH_3. These materials were collected after quenching the reaction at (a) 230, (b) 320, (c) 390, (d) 490, (e) 650, and (f) 800°C, respectively. The heating rate was 60°C/h.

is schematically illustrated in Fig. 6. The materials were held at the final temperature for 1 h then rapidly cooled to room temperature and passivated. We chose intermediate temperatures of 410 and 510°C, and a final temperature of 660°C. The intermediate temperatures were sufficient to complete the conversions of V_2O_5 to VO_2 and VO_2 to V_2O_3, respectively, at both heating rates. The final temperature was selected based on the results of screening experiments. Holding the materials at a final temperature of 660°C for 1 h was sufficient to produce VN at both of the heating rates. Temperatures lower than 640°C were not sufficient to produce the nitride even at the lower heating rate.

Results of the experiments are summarized in Table 3. All of the materials were phase-pure VN based on XRD. The BET surface areas ranged from 49 to 59 m^2/g (materials reduced at 500°C for 3 h in H_2). Slower heating

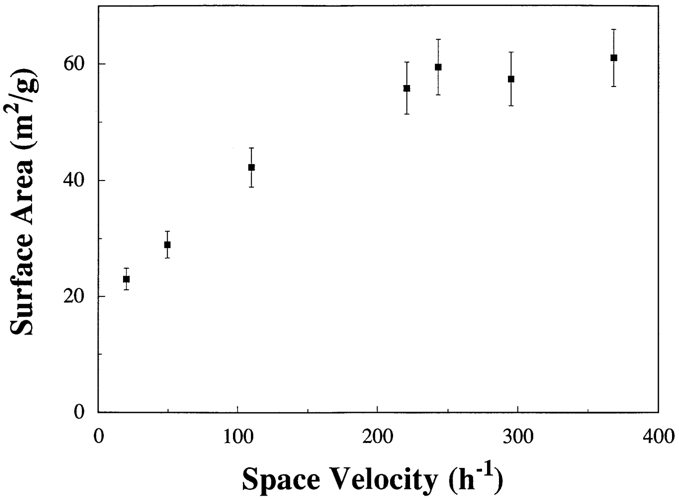

FIG. 4. Effect of the molar hourly space velocity on the vanadium nitride surface areas. The oxides were reacted with NH_3 as the temperature was increased from room temperature to 660°C at 60°C/h.

TABLE 3

Effect of Heating Rates on Properties of the Vanadium Nitrides[a]

Catalyst code	Heating rate (°C/h) β_1	β_2	β_3	Surface area[b] (m^2/g)	Crystallite size (nm)
VN+++	180	180	180	50	14
VN++−	180	180	60	51	13
VN+−+	180	60	180	52	13
VN+−−	180	60	60	55	12
VN−++	60	180	180	49	14
VN−+−	60	180	60	58	14
VN−−+	60	60	180	54	13
VN−−−	60	60	60	59	13

[a] The space velocity for these experiments was 300 h^{-1}.

[b] Measured after reduction in flowing H_2 at 500°C for 3 h.

rates in all heating segments resulted in higher surface areas; however, the effect was small. Differences between the crystallite sizes were also minor. The mean pore diameters and pore size distributions for all eight materials were not significantly different. In conclusion, the heating rate had a relatively small effect on microstructures of the vanadium nitrides. This behavior contrasts that observed during the production of other early transition metal nitrides including molybdenum nitrides. The differing effects of the heating rates may have been a consequence of the different reaction pathways. The TPR of MoO_3 with NH_3 involved parallel solid-state reactions (1, 24). The selectivity to these reactions and surface areas of the products were functions of the heating rates. In particular, when the nitridation of MoO_3 proceeded through MoO_2, the resulting surface area was low (<20 m^2/g). When the reaction proceeded through H_xMoO_3 ($x \leq 0.3$), the nitride had a high surface area (>100 m^2/g). Because the TPR of V_2O_5 proceeded via series reactions we believe the opportunity to direct the reaction pathway was not available and the surface areas were not significantly affected by changing the heating rates.

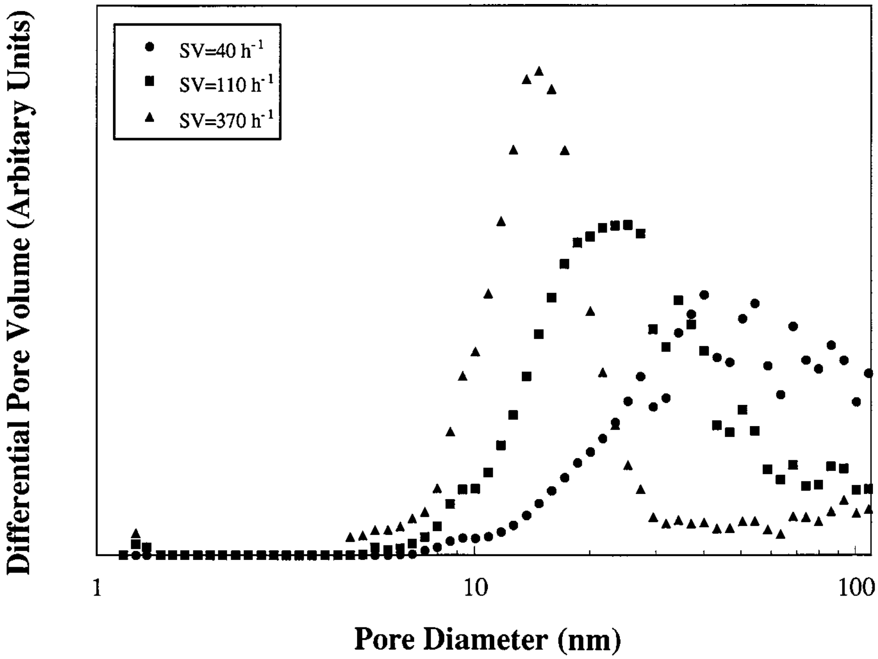

FIG. 5. Pore size distributions for vanadium nitrides prepared using different molar hourly space velocities (SV). The oxides were reacted with NH_3 as the temperature was increased from room temperature to 660°C at 60°C/h.

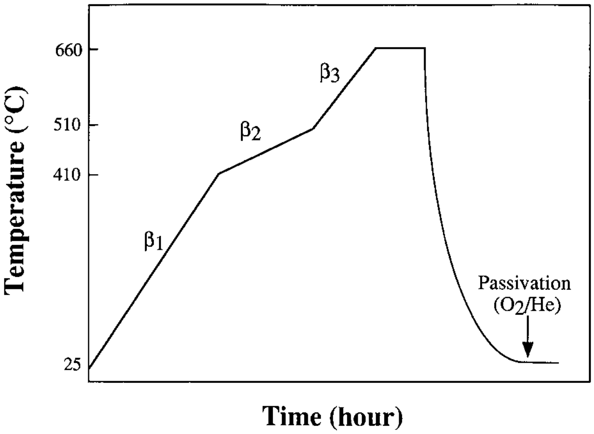

FIG. 6. Schematic of the temperature program used to prepare high surface area vanadium nitrides from V_2O_5. The heating rates were 60 or 180°C/h.

Effect of Reduction Conditions on the Surface Areas and Oxygen Uptakes

The vanadium nitrides were passivated so that they could be transferred to other systems (e.g., catalytic reactor) without experiencing bulk oxidation. Passivation is known to modify the surface properties of early transition metal nitrides and carbides (23). Prior to measurement of the adsorptive and catalytic properties, the passivation layer is typically removed by pretreating the material in H_2. Temperature-programmed reduction spectra for one of the passivated vanadium nitrides are illustrated in Fig. 7. The surface area of this material was 23 m^2/g prior to reduction. Results for the other materials were similar. The desorption of H_2O, NH_3, and a small amount of N_2 occurred at ≈150°C. The consumption of H_2 and concomitant production of H_2O occurred at ≈480°C. No other H_2O peaks were observed at higher temperatures. Small amounts of NH_3 and N_2 were also detected at ≈480°C. These compounds could result from the reduction of VN to vanadium metal and/or from the desorption or decomposition of chemisorbed NH_3. There were no significant changes in the mass spectrometer or TCD signals while maintaining the material in H_2 at 600°C. The effects of reduction temperature on the surface area and O_2 uptake were further demonstrated by reducing the materials at various temperatures for 3 h (Table 4). Reduction at temperatures less than 500°C was not sufficient to maximize the oxygen uptake and completely remove the passivation layer. These results along with those from the TPR experiments suggested the use of a temperature of 500°C to remove the passivation layer from the nitride surfaces.

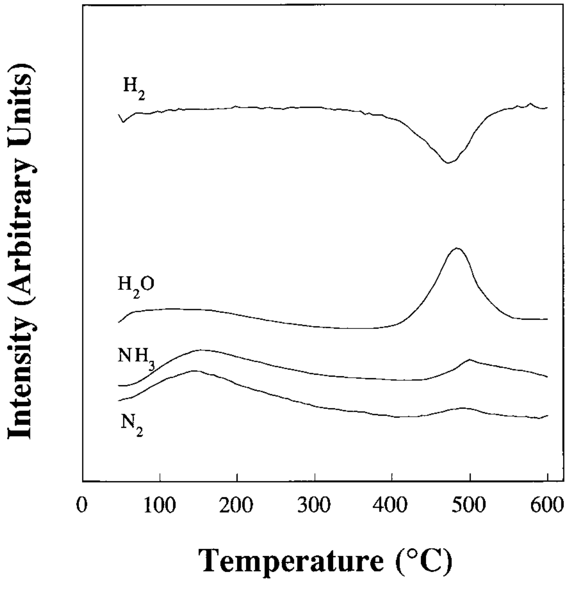

FIG. 7. Temperature-programmed reduction spectra for a passivated vanadium nitride. The surface area of this material was 23 m^2/g prior to reduction. The heating rate was 5°C/min.

The effects of reduction time on the surface areas and O_2 uptakes were investigated for several of the vanadium nitrides. The reduction temperature was set at 500°C. Results for an intermediate surface area nitride are illustrated in Fig. 8. The other materials behaved in a similar manner. The BET surface area and oxygen uptake increased to a maximum at 3 h and then decreased slightly. Note that changes in the BET surface area were not as significant as changes in the O_2 uptake indicating that the passivation layer had differing effects on the total and specific surface areas. We believe the presence of oxygen in or on the passivated surface inhibited O_2 chemisorption while N_2 physisorption was not significantly affected. A 3 h reduction at 500°C appeared to be sufficient to maximize the oxygen uptake and reduce the passivation layer.

The relative amount of oxygen that chemisorbed was similar for all of the vanadium nitrides after reduction

TABLE 4

Effect of Reduction Temperature on Surface Characteristics of the Vanadium Nitrides

Sample code	Reduction temperature[a] (°C)	Surface area[b] (m^2/g)	O_2 uptake[b] (μmol O_2/g)
VN-14	400	12	0
	500	14	45
	600	14	39
VN-29	400	28	15
	500	32	109
	600	30	113
VN-59	400	59	177
	500	55	248
	600	52	244

[a] Materials were reduced for 3 h in flowing H_2.

[b] The BET surface area and O_2 uptake were reproducible to within ±10% and ±15%, respectively.

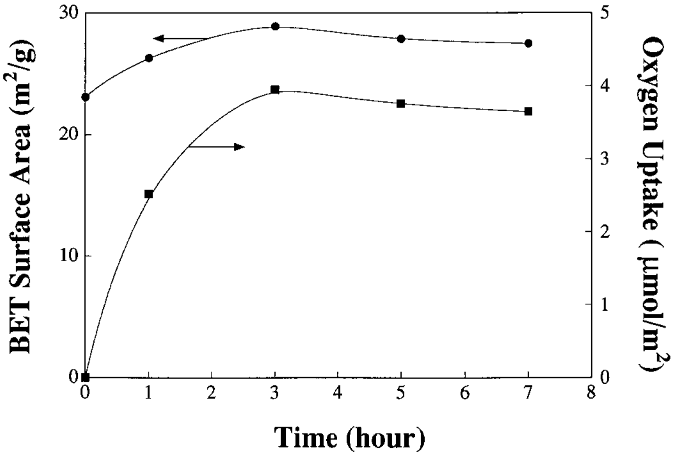

FIG. 8. The effect of reduction time on the surface areas and O_2 uptakes of an intermediate surface area passivated vanadium nitride. The reduction temperature was 500°C.

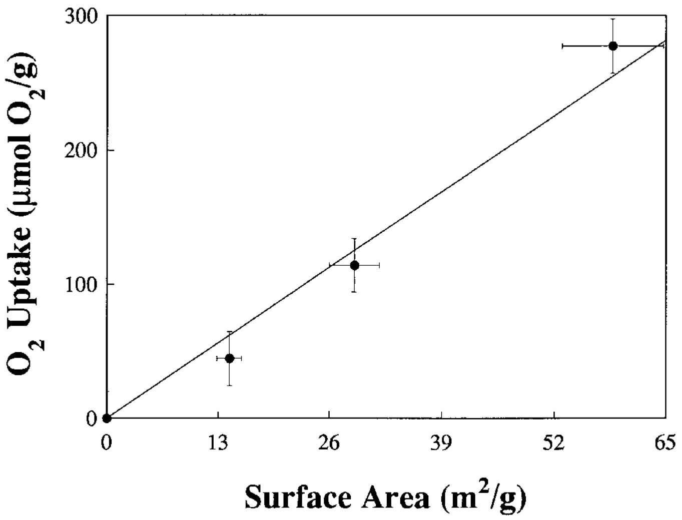

FIG. 9. Relationship between the O_2 uptakes and BET surface areas for the vanadium nitrides. The passivated vanadium nitrides were reduced for 3 h in flowing H_2 at 500°C prior to the O_2 uptake and BET surface area measurements.

in H_2 at 500°C for 3 h. This suggested that their surface chemistries were similar. A straight line adequately represents the relationship between the O_2 uptake and surface area (Fig. 9). The slope of the line corresponds to a site density of 2.8×10^{14} O_2/cm^2. Assuming that O_2 dissociates and the surface metal atom density for VN is 10^{15} V/cm^2, the average oxygen uptake corresponds to an $O/V_{surface}$ ratio of 0.56. This is slightly higher than $O/Mo_{surface}$ ratios that we observed for γ-Mo_2N (1) and α-Mo_2C (28) (0.21 and 0.13, respectively) and suggests that one oxygen atom coordinated to approximately two surface vanadium atoms. The O/V stoichiometry observed here is substantially higher than the CO/V stoichiometry of 0.07 reported by Oyama and co-workers (13) although they reduced their materials at lower temperatures for shorter times (450°C for 2 h). It is also possible that either O/V and CO/V stoichiometries for the catalysts were different, or oxygen and CO adsorbed onto different sites.

Catalytic Properties

The butane activation rates and product selectivities were measured for selected vanadium nitrides after reduction in H_2 at 500°C for 3 h. The reaction rates at 450°C are summarized in Table 5. The gravimetric and volumetric rates are the reaction rates normalized by the catalyst weight and volume, respectively. The catalyst code includes the surface area which ranged up to ≈60 m^2/g. For example, VN-14 had a BET surface area of 14 m^2/g. For comparison, butane conversion rates for a tungsten carbide and a Pt–Sn/Al_2O_3 catalyst containing 0.3% Pt, 1.2% Sn, and 1.8% Na (29) are included in Table 5. The WC and Pt–Sn/Al_2O_3 catalysts were pretreated in H_2 for 3 h at 480°C. These conditions were determined from temperature-programmed reduction experiments (6). No significant change in the reaction rate was observed when the flow rate was changed or the catalyst particles were ground confirming the absence of external transport limitations. The reaction rates reached steady-state after approximately 1 h on-stream and were reproducible to within ±10% during subsequent runs. The nitrides showed negligible deactivation after more than 40 h on stream.

TABLE 5

Butane Conversion Reaction Rates for the Vanadium Nitride, Tungsten Carbide, and Pt–Sn/Al_2O_3 Catalysts

Catalyst	Gravimetric reaction rates[a] (nmol/g s)				Volumetric reaction rates (nmol/cm^3 s)
	Dehydrogenation	Isomerization	Hydrogenolysis	Total	
VN-14	89	<0.1	<0.1	89	267
VN-29	166	0.3	1.1	167	501
VN-59	253	1.0	3.0	257	771
WC-12	365	25	750	1141	8900
Pt–Sn/Al_2O_3	350	1.1	2.9	354	690

[a] Measured under differential conditions at 450°C and 101 kPa for a reactant mixture containing 4% C_4H_{10}, 60% H_2, and 36% He.

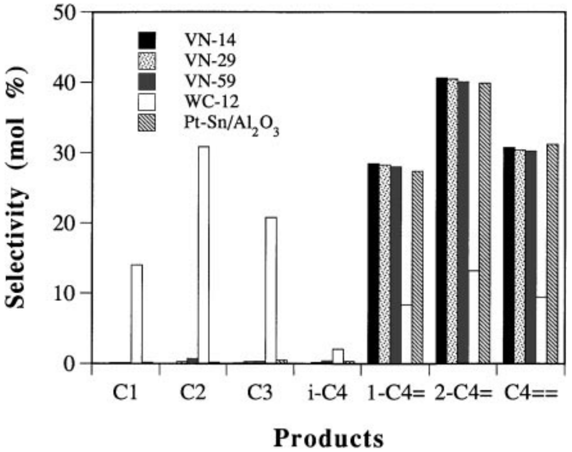

FIG. 10. Butane conversion selectivities measured at 450°C and 101 kPa. The abbreviations C1, C2, C3, i-C4, 1-C4=, 2-C4=, and C4== represent CH_4, the total of C_2H_4 and C_2H_6, the total of C_3H_6 and C_3H_8, i-C_4H_{10}, 1-C_4H_8, 2-C_4H_8, and 1,3-C_4H_6, respectively.

Steady-state gravimetric reaction rates for the nitrides depended on the surface area and were lower than those for the Pt–Sn/Al_2O_3 catalyst; however, volumetric rates for the VN-59 catalyst were superior to those for the Pt–Sn/Al_2O_3 catalyst. This advantage is primarily a consequence of the density of VN being much higher than that for Al_2O_3. A density of 3.9 g/cm^3 was assumed for the Pt–Sn/Al_2O_3 catalyst and the void fraction for all of the materials was estimated to be 0.5. The enhanced volumetric reaction rate has significant practical implications as catalytic reactors are often designed based on volume. Reaction rates and activities for the vanadium nitrides were lower than those for the tungsten carbide; however, the vanadium nitrides were far more selective. At least three types of reactions are possible during butane conversion; dehydrogenation to butenes and butadiene, isomerization to isobutane and isobutene, and/or hydrogenolysis to lighter hydrocarbons. The vanadium nitrides possessed excellent selectivities toward dehydrogenation products (Fig. 10). The predominant product was *cis*-2-C_4H_8 and selectivities to *trans*-2-C_4H_8 were less than 1%. The butane dehydrogenation selectivities were greater than 98% and essentially independent of surface area. The vanadium nitrides produced approximately the same product distribution as the Pt–Sn/Al_2O_3 catalyst. Considering the cost and complexity of manufacturing supported Pt–Sn, vanadium nitrides are attractive candidates for development as alkane dehydrogenation catalysts. Unlike the vanadium nitride and Pt-based catalysts, the tungsten carbide catalyst produced significant amounts of hydrogenolysis and isomerization products. We believe differences between catalytic properties of the vanadium nitrides and tungsten carbide were due to differences between their electronic properties, in particular their ionicities (30).

Butane dehydrogenation rates for the vanadium nitrides increased almost linearly with the surface area and O_2 chemisorptive uptake. The slope of a plot of the gravimetric reaction rate versus the surface area yields an average activity of 4.3 nmol/m^2 s at 450°C. Assuming a site density of 10^{15} sites/cm^2, this activity corresponds to a turnover frequency of 2.6×10^{-4} s^{-1}. The oxygen uptake normalized reaction rates allow a comparison of the intrinsic catalytic properties of the VN and Pt-based catalysts. Oxygen did not adsorb to the Al_2O_3 indicating that oxygen uptake for the Pt–Sn/Al_2O_3 catalyst was due to chemisorption on Pt and/or Sn. The average turnover frequency was 4.3×10^{-4} s^{-1} at 450°C for the VN catalysts assuming that oxygen chemisorbed atomically onto the active sites. For comparison the turnover frequency for the Pt–Sn/Al_2O_3 catalyst was 2.5×10^{-2} s^{-1} again assuming that oxygen chemisorbed atomically onto the active sites. Because oxygen may have chemisorbed onto Sn, 6.3×10^{-2} s^{-1} should be considered as a minimum value for the turnover frequency for Pt in the Pt–Sn/Al_2O_3 catalyst. Clearly intrinsic activities for the Pt–Sn catalyst were superior to those for the VN catalysts.

The linear relationship between the butane activation rate and surface area implied that this reaction was structure-insensitive over the vanadium nitrides. Structure-insensitivity is not surprising for materials that selectively catalyze dehydrogenation reactions (31). This type of behavior was also observed for higher surface area vanadium nitrides. The surface area normalized butane dehydrogenation rates for VN catalysts (>200 m^2/g) prepared from oxide aerogels were similar to those reported in this paper (14). In contrast, surface area normalized butane conversion rates for a series of tungsten carbides were strong functions of their morphologies and crystalline structures (6). These materials had high selectivities toward hydrogenolysis products. Hydrogenolysis reactions are known to be structure-sensitive over other types of catalysts including the Pt-group metals (31, 32).

Apparent activation energies for vanadium nitrides with different surface areas were within experimental error of each other suggesting that the materials shared the same reaction mechanism. The vanadium nitrides had higher activation energies (37 ± 1 kcal/mol) than that of the Pt–Sn/Al_2O_3 catalyst (28 ± 1 kcal/mol). This result indicates that kinetics of the elementary reactions or reaction mechanisms for the VN and Pt-based catalysts were different. The magnitude of the activation energies also suggested that internal mass transfer did not limit the reaction rates.

SUMMARY

Mesoporous vanadium nitrides with surface areas up to 60 m^2/g were prepared by the TPR of V_2O_5 (7 m^2/g) with flowing NH_3. X-ray diffraction and TGA indicated

that the solid-state reaction proceeded via sequential reduction of the oxide followed by nitrogen incorporation. The reaction pathway to VN was as follows: $V_2O_5 \rightarrow V_4O_9 \rightarrow VO_2 \rightarrow V_2O_3 \rightarrow VO_{0.9} \rightarrow VN$. While changing the heating rates resulted in minor changes in the vanadium nitride microstructures, changing the space velocity had a very significant effect on the surface area, crystallite size, pore size distribution, and surface morphology. The higher space velocities resulted in the formation of higher surface area vanadium nitrides with smaller crystallites and narrower, more uniform pores. Scanning electron microscopy also showed a decrease in grain size as the space velocity was increased. The speed with which H_2O and other solid-state reaction by-products were removed from the surface was considered to be a key reason for variations in the surface microstructures. To maximize the surface area and O_2 chemisorptive uptake, the passivated VN catalysts had to be reduced in H_2 at 500°C for 3 h. The resulting materials were able to chemisorb $\approx$0.6 oxygen atoms for every surface vanadium atom.

The vanadium nitrides were stable and highly active butane dehydrogenation catalysts, with selectivities greater than 98%. The reaction rates increased almost linearly with surface area yielding an average activity of 4.3 nmol/m^2 s at 450°C. The oxygen uptake based turnover frequency was 4.3×10^{-4} s^{-1} compared to a value of 6.3×10^{-2} s^{-1} for the Pt–Sn/Al_2O_3 catalyst. There were no significant changes in selectivities among nitrides with different surface areas. While reaction selectivities for the nitrides were very similar to that of the Pt–Sn/Al_2O_3 catalyst, the apparent activation energies were different. This suggested that there were substantial differences between catalytic properties of the VN and Pt-based catalysts.

ACKNOWLEDGMENTS

The authors thank the National Science Foundation Presidential Young Investigator Program (CTS-9158527) for financial support of this research and Amoco Oil Company for supplying the Pt–Sn/Al_2O_3 catalyst. Contributions from the Micromeritics Company are also acknowledged.

REFERENCES

1. Choi, J., Brenner, J. R., Colling, C. W., Demczyk, B. G., Dunning, J., and Thompson, L. T., *Catal. Today* **15**, 201 (1992).
2. Sajkowski, D. J., and Oyama, S. T., *ACS Prep. Div. Petrol. Chem.* **35**(2), 233 (1990).
3. Schlatter, J. C., Oyama, S. T., Metcalfe III, J. E., and Lambert, J. M., Jr., *Ind. Eng. Chem. Res.* **27**, 1648 (1988).
4. Leclercq, L., Imura, K., Yoshida, S., Barbee, T., and Boudart, M., *in* "Preparation of Catalysts II" (B. Delmon, Ed.), p. 627, Elsevier, New York, 1978.
5. Volpe, L., and Boudart, M., *J. Phys. Chem.* **90**, 4874 (1986).
6. Curry, K. E., Ph.D. dissertation, University of Michigan, 1995.
7. Neylon, M. K., Choi, S., Kwon, H., Curry, K. E., and Thompson, L. T., *Appl. Catal.*, in press.
8. Levy, R. B., and Boudart, M., *Science* **181**, 547 (1973).
9. Chen, J. G., Fruhberger, B., Weisel, M. D., Baumgartner, J. E., and De Vries, B. D., *in* "Chemistry of Transition Metal Carbides and Nitrides" (S. T. Oyama, Ed.), p. 439 , Blackie, Glasgow, U.K., 1996.
10. Boudart, M., Oyama, S. T., and Volpe, L., U.S. Patent 4,515,763, 1985.
11. Ribeiro, F. H., Dalla Betta, R. A., Guskey, G. J., and Boudart, M., *Chem. Mater.* **3**, 805 (1991).
12. Volpe, L., Oyama, S. T., and Boudart, M., *in* "Preparation of Catalysts III" (P. Grange and P. A. Jacobs, Eds.), p. 147, Elsevier Science, Amsterdam, 1983.
13. Kapoor, R., and Oyama, S. T., *J. Solid State Chem.* **99**, 303 (1992).
14. Kwon, H., Ph.D. dissertation, University of Michigan, 1998.
15. Lastoskie, C., Gubbins, K. E., and Quirke, N., *Langmuir* **9**, 2693 (1993).
16. Lastoskie, C., Gubbins, K. E., and Quirke, N., *J. Phys. Chem.* **97**, 4786 (1993).
17. Oliver, J. P., and Conklin, W. B., "International Symposium on the Effects of Surface Heterogeneity in Adsorption and Catalysis on Solids," Kazierz Dolny, Poland, July 1993.
18. Choi, J.-G., Lee, H. J., and Thompson, L. T., *Appl. Surf. Sci.* **78**, 299 (1994).
19. Cullity, B. D., "Elements of X-Ray Diffraction," Addison–Wesley, Reading, MA, 1978.
20. McClune, W. F. (Ed.), "Powder Diffraction Files," International Center for Diffraction Data, Swarthmore, PA 1991.
21. Weast, R. C. (Ed.), "CRC Handbook of Chemistry and Physics," 58th ed., CRC Press, Boca Raton, FL, 1977.
22. Oyama, S. T., Kapoor, R., Oyama, H. T., Hofmann, D. J., and Matijevíc, E., *J. Mater. Res.* **8**, 1450 (1993).
23. Choi, J. G., Ph.D. dissertation, University of Michigan, 1992.
24. Jaggers, C. H., Michaels, J. N., and Stacy, A. M., *Chem. Mater.* **2**, 150 (1990).
25. Mulfinger, H. O., *J. Am. Ceram. Soc.* **49**, 462 (1966).
26. Brinker, C. J., *J. Am. Ceram. Soc.* **65**, C4 (1982).
27. Anderson, P. J., and Morgan, P. L., *Trans. Faraday Soc.* **60**, 930 (1964).
28. Choi, J., Brenner, J. R., and Thompson, L. T., *J. Catal.* **154**, 33 (1995).
29. The Pt–Sn/Al_2O_3 catalyst was provided by the Amoco Oil Company.
30. Gubanov, V. A., Ivanovsky, A. L., and Zhukov, V. P., "Electronic Structure of Refractory Carbides and Nitrides," Cambridge Univ. Press, Cambridge, MA, 1994.
31. Boudart, M., and Djéga-Mariadassou, G., "Kinetics of Heterogeneous Catalytic Reactions," Princeton Univ. Press, Princeton, NJ, 1984.
32. Somorjai, G. A., "Introduction to Surface Chemistry and Catalysis," Wiley, New York, 1994.